



Preliminary Assessment of the Operational Dam's Performance in November 12, 2017 Sarpol-e Zahab Earthquake

Abdollah Sohrabi-Bidar^{1*}, Farhad Imanshoar², Shahram Maghami³,
and Malek-Mirza Darvishi⁴

1. Associate Professor, School of Geology, College of Science, University of Tehran, Tehran, Iran, * Corresponding Author; email: asohrabi@ut.ac.ir

2. Ph.D. of Civil Engineering, Iran Water Resource Management Company, Iran

3. Ph.D. Student, School of Geology, College of Science, University of Tehran, Tehran, Iran

4. M.Sc. Graduate of Civil Engineering, Kermanshah Regional Water Company, Kermanshah, Iran

Received: 18/08/2018

Accepted: 10/10/2018

ABSTRACT

Following the November 12, 2017 Sarpol-e Zahab earthquake with a magnitude of 7.3 in Richter scale, emergency inspection of dams has been performed for dams located at the epicentral distance of 125 km, according to the ICOLD recommendations. In the mentioned zone, there are 16 impounded operational storage dams. Inspected dams had no apparent significant damages and only some thin cracks had been observed in Tange-Hamam Dam that is a non-homogenous embankment dam and the closest operational dam to the epicenter of the earthquake, with a distance of 25 km from the epicenter. There were some defects such as longitudinal cracks and some tiny transversal cracks on the crest of the dam as well as some vertical cracks in the spillway's left approach wall. Regarding the observed evidence, more precise investigations of the dam behavior were performed through the instrumentation data. Settlement measuring on magnetic plates shows the settlement of 13 cm near the embankment surface at the middle of the dam crest, which is about 0.22 of the dam height. This rate of strain has been compared with some published international experiences, which generally shows the acceptable performance of the dam. To ensure the safety of the dam, monitoring of all instruments should be continued, as well as the precise geodetic measuring in the dam body, which is in progress now.

Keywords:

Sarpol-e Zahab earthquake;
Tange-Hamam Dam;
Instrumentation data;
Dam settlement

1. Introduction

Surface water containment by building small and large dams along with their benefits is considered as a threat to societies due to the huge volume of accumulated water behind them. Historical Accidents and failures of dams confirm the importance of paying attention to their safety in both static and dynamic situations. Several experiences of dams' damages due to earthquake events have been published. Perhaps the oldest reports are about Augusta Dam in the state of

Georgia, which affected by the Charleston 1886 earthquake with an estimated magnitude of 7.5 [1]. During this earthquake, the dam was broken down and the resulting flood drowned residential areas. The American National Dams Committee has compiled a collection of dams affected by earthquakes in three studies [2-4]. Tani [5] has also summarized and presented the effects of earthquakes on the earth dams in Japan. Among the storage earthen dams, the Sheffield Hydraulic dams and the Lower

San Fernando dam in the United States and the Chang and Shivilakha dams in India are indicative of the extent of injuries and the level of damages due to huge earthquake occurrences.

The Sheffield Dam was a relatively small dam with a height of 7.6 meters, which collapsed during the 1925 Santa Barbara earthquake with the magnitude of 6.2 in California, USA. The main cause of the collapse of the dam was liquefaction phenomenon in the foundation and the body of the dam that was mainly composed of Silty-Sand or Sandy-Silt [6]. The Lower San Fernando Dam, which was failed during 1971 San Fernando earthquake with a magnitude of 6.7 in California, was a 43-meter height dam that was mainly constructed by Silty-Sand and Sandy-Silt materials. The water level was 11 meters lower than the crest of the dam during the earthquake. Due to liquefaction in the dam body, large pieces of materials start moving upward on the liquefied parts, in a way that the distance between reservoir water level and embankment crest became about 1 meter [7-9]. The 2001 Bhuj earthquake in India, with a magnitude of 7.9, caused partial or total failure in six embankment dams in India, among which Chang and Shivilakha dams faced with total damages. Chang Dam was an earthen dam with 15.5 m height, which after about 4 m settlement and more than 7 m horizontal displacement, eventually collapsed. Shivilakha Dam was also a 18 m earthen dam which faced with a 2 m settlement and 1.2 m horizontal displacement. The main cause of damages in these dams was reported as the liquefaction phenomenon in loose materials of the alluvial basement [10-11]. In 2011 Tohoku earthquake with a magnitude of 9.0, inspections of 300 dams in the affected area, revealed damages to about 10 percent of the dams [12]. During the 2008 Wenchuan earthquake in China with a magnitude of 8.0, about 2666 dams encountered damages, among them 66 dams faced the danger of complete collapse [13]. Among damaged dams, Zipingpu high elevated Dam was the most important one, with 156 m height, located at a 17 km distance to the earthquake epicenter. The dam experienced 70 cm settlement caused extensive cracks on the dam concrete face [14].

Past experiences identified the safety assessment of dams based on three components of structural

health, continuous monitoring of dam behavior and readiness to deal with emergencies [15-16]. Structural health is related to design and construction in accordance with updated standards as well as proper maintenance of the structure during the operation period. Monitoring the behavior of the dam could be achieved by various processes such as visual inspection and quantitative measurements and instrumentation data interpretations. Emergency preparedness is also the third pillar of safety, which includes a set of processes and preparations after the critical conditions in a dam. Earthquake events, along with some other phenomena such as large floods or long-term rainfall, are one of the factors that cause emergency situations and require special inspections and monitoring of dams.

This study presents the results of preliminary assessments of the performance of operational storage dams after November 12, 2017, Sarpol-e Zahab earthquake with a magnitude of 7.3. In this research, the results of emergency inspections of 16 dams were presented and in particular, the settlement behavior of the Tange-Hamam Dam at a distance of about 25 km from the earthquake epicenter is investigated.

2. Iranian Dams and Monitoring After the Earthquake

Iran has a long history of constructing water work structures, and some of the old dams constructed in Iran have been used up to recent years, including the Kurit dam with a height of 60 meters [17]. One of the main reasons for the development of dams and other water supply structures is resource constraints, climatic conditions, and disproportionate distribution of temporal and spatial rainfall along with the need for water supplies. At present, about 650 large dams are in operation, construction and study in Iran, in accordance with the definition of the International Commission on Large Dams, in which about 260 dams are in operation, 130 dams are under construction, and 260 dams are in the study.

The distribution of dams is proportional to the abundance of water resources; and therefore, they are generally concentrated in mountainous and highland areas. This issue has inevitably caused the proximity of these facilities to seismic resources.

Many of the country's dams have been erected in high seismic hazard areas. Although there are strong and well-established rules in the design of dams [18], past experience of earthquakes has always brought new wonders and surprises. With respect to the importance of the dam's safety, there should always be a good preparation for an earthquake in them.

Figure (1) shows the distribution map of the dams in operation and construction in Iran as well as the location of major faults in the country [19-20]. The map also shows the relative seismic hazard of Iran [21]. Accordingly, none of the dams is located in a relatively low hazard zone, and only 10% of the dams are located in a relatively moderate hazard zone. More than 70% of them are located in the zones of relatively high hazard and close to 20% are constructed in very high hazard areas.

Typically, the process of monitoring of operating dams, including minimum monthly inspections and annual interpretation of quantitative instrumentation data. Besides, a comprehensive safety assessment of dams is recommended to be done every 5 to 10 years depending on the importance of the dam, because of changes in the conditions of the site and the dam itself and also the changes of criteria etc. In

an emergency situation of an earthquake event, International Commission on Large Dams recommended conducting emergency inspections in dams located within a certain radius of the epicenter, based on the magnitude of the earthquake, in accordance with Table (1) [22]. In addition, a detailed inspection checklist [23] was proposed to guide and accurately examine the status of the inspected dam. Conditional on non-observance of major anomalies, emergency monitoring is carried out within 24 hours of the earthquake, 72 hours after the earthquake, and will continue for a month after the earthquake. In cases of observing abnormal behavior, the monitoring frequencies will be increased commensurate with the observed abnormality.

Table 1. Recommendations of the International Commission on Large Dams for post-earthquake inspections [22-23].

Magnitude (Richter)	Distance (Km)
≥ 4	≤ 25
≥ 5	≤ 50
≥ 6	≤ 80
≥ 7	≤ 125
≥ 8	≤ 200

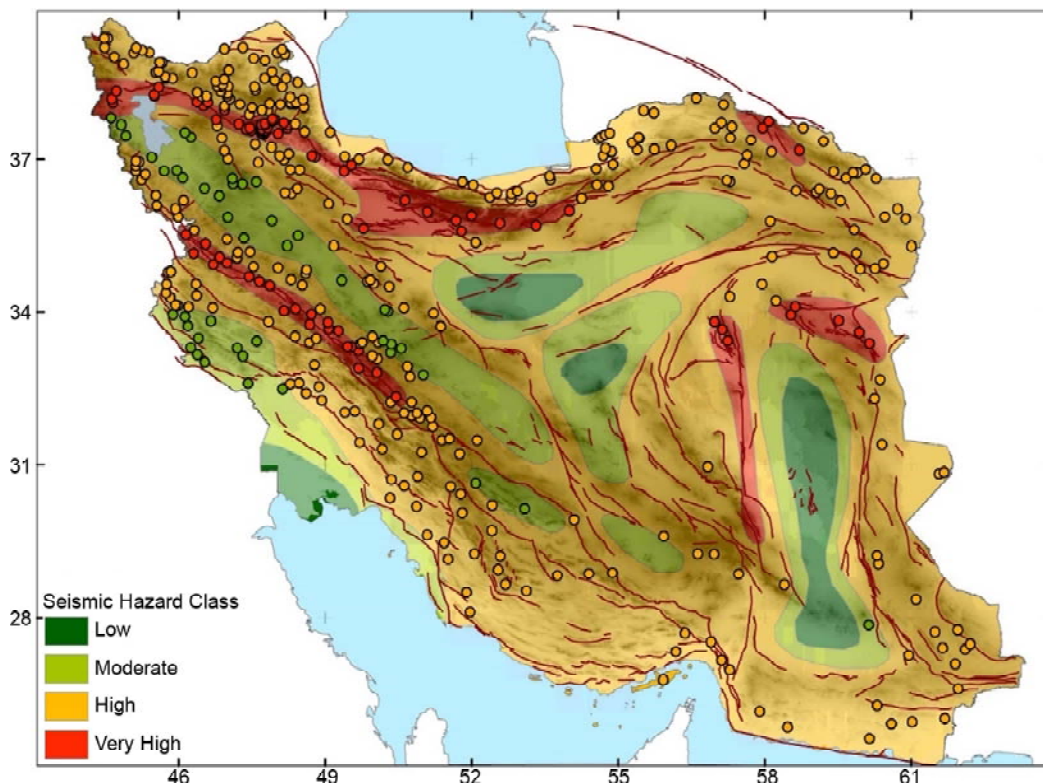


Figure 1. Map of dam's locations and relative seismic hazard zones in Iran.

3. The Performance of Dams Located in the Sarpol-e Zahab Earthquake Area

At 21:48 local time on November 12, 2017, an earthquake event with a magnitude of 7.3 occurred near Ezgeleh city, Kermanshah province, Iran. The earthquake has been initially located at a longitude of 45.90 and a latitude of 34.84, which then was relocated to a longitude of 45.76 and a latitude of 34.77 [24]. The earthquake followed up by a large number of aftershocks up to a magnitude of 6.0. Based on the initial location, the nearest cities to the earthquake epicenter were Ezgeleh, 5 km away, Tazeh-Abad 25 km away and Bayangan 37 km away.

Due to the magnitude of the earthquake and based on the recommendations of the ICOLD, dams located within a radius of 125 km from the epicenter of the earthquake were subject to emergency inspections. Accordingly, the list of operational impounded dams located in the affected area was extracted. Figure (2) illustrates the position map of the operational dams in the area affected by the earthquake. There were 16 operational dams in the area, all earth-fill and rock-fill embankments, which were subjected to emergency inspections. Table (2) shows the characteristics of these dams and the distance to the earthquake epicenter based on the initial location by the Iranian Seismological

Center (IRSC). As it can be seen, the Tange-Hamam Dam with a distance of 35 km is the nearest dam to the earthquake epicenter. The distance reduced to less than 25 km after more detailed determination of epicenter location.

In the initial observations, no significant damages were observed in the dam's bodies, and only a few cases of cracking have occurred in dams near the seismic epicenter, especially the Tange-Hamam Dam. In this regard, recommendations were made to monitor the status of the cracks. According to the instrumentation data, except for some few cases near the epicenter that shows a small increase in the pore pressure, no significant phenomenon observed. Although, yet continuous monitoring is required to achieve more accurate evaluations. At a distance of 4 km downstream of the Kangir Dam, located 105 km from the earthquake epicenter, inflorescence was observed in a fountain, which monitoring of the flow situation of the spring ordered based on the agenda. In general, early post-earthquake assessments did not show significant concern associated with dams and related structures. Further assessments of the cracks conditions in the inspected dams also indicate stagnation and lack of growth. The pollution of the Kangir Dam downstream fountain was gradually faded within a week after the earthquake.

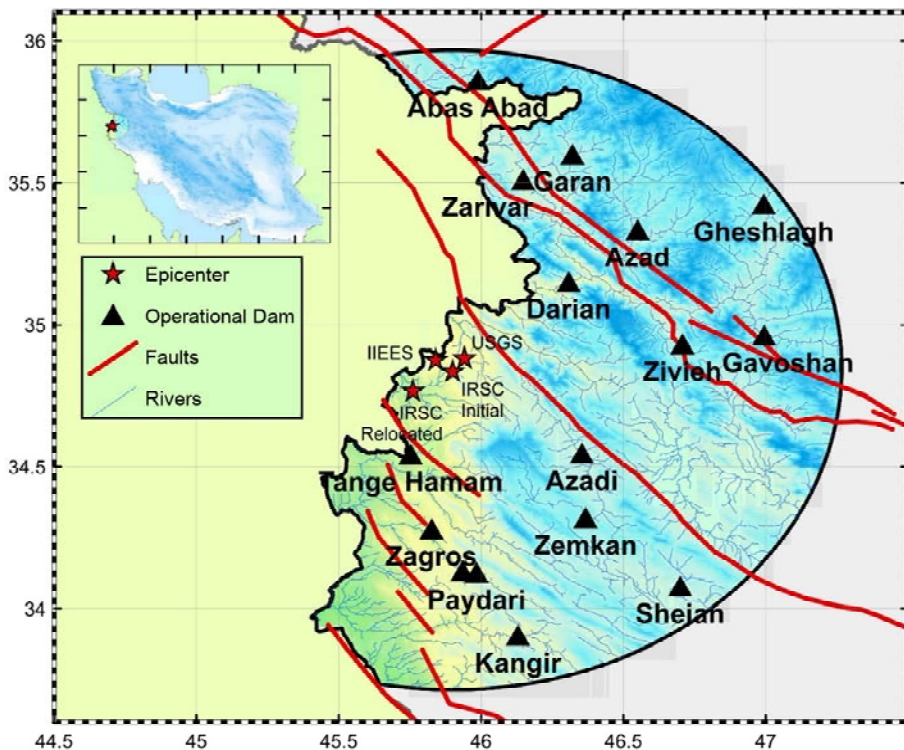


Figure 2. Location of operational dams in the earthquake affected area.

Table 2. Characteristics of operational dams in the earthquake affected area.

No.	Name	Operating Organization	Volumetric Impound Rate	Height (m)	Volume (Mm ³)	Distance to Epicenter (Km)*
1	Tange-Hamam	¹ KSHRW	78%	56	67	35
2	Darian	² IWPCCO	89%	146	338	50
3	Azadi	KSHRW	45%	56	71	53
4	Zagros	KSHRW	79%	47	60	60
5	Zemkan	KSHRW	17%	56	23	70
6	Zivieh	³ KDRW	79%	48.2	17	75
7	Gilan-e Gharb	KSHRW	36%	15	6.7	78
8	Zarivar	KDRW	69%	4	58	78
9	Azad	IWPCCO	27%	118	300	80
10	Paydari	KSHRW	46%	48	17	80
11	Garan	KDRW	83%	58.5	92	93
12	Gavoshan	KSHRW	91%	116	554	100
13	Kangir	⁴ ILRW	67%	38.5	19	105
14	Sheian	KSHRW	43%	20.5	9	110
15	Abbas Abad	KDRW	20%	49	14	115
16	Gheshlagh	KDRW	77%	80	224	120

*Distance is based on the initial location of the earthquake epicenter by IRSC

¹ KSHRW=Kermanshah Regional Water Authority

² IWPCCO= Iran Water and Power Resources Development Company

³ KDRW=Kurdistan Regional Water Authority

⁴ ILRW= Ilam Regional Water Authority

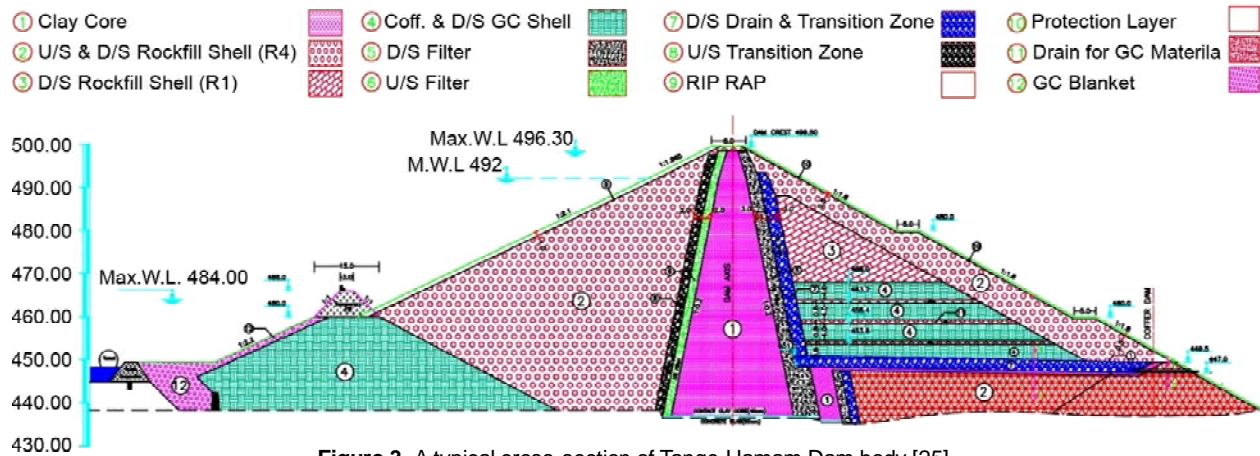


Figure 3. A typical cross-section of Tange-Hamam Dam body [25].

4. Performance of Tange-Hamam Dam during the Earthquake

Tange-Hamam Dam was the nearest dam to Sarpol-e Zahab earthquake epicenter. The dam located 17 km east of Qasr-e Shirin city on the Ghuretu River. The first phase studies of the dam began in 2002 and the second phase studies ended in 2005. The embankment operations of the dam structure began in 2010 and ended in spring of 2013 and impoundment has been started. After the earthquake of Sarpol-e Zahab, due to the low distance of the dam site to earthquake epicenter, visual examinations and settlement measurements have been carried out and the results have been analyzed.

4.1. Specifications of Tange-Hamam Dam

Tange-Hamam is an earthen-rock fill dam with a

vertical clay core. Figure (3) shows the cross-section of the body of the dam. The height of the dam is 60 m to the basement, crest length is 437 m and crest width is 8 m. Elevation of the crest of the dam is 499.5 m and normal operating level of the reservoir is 492 m with respect to the mean sea level. Reservoir volume in normal level is 67 Mm³. Dam's upstream and downstream face slip is 1:2.1 and 1:1.8, respectively.

The dam site is geologically located in the Zagros zone and is located almost on the border of the mountain and plain. The area is mainly constructed of the Pliocene conglomerate of Bakhtiari Formation, which has a gentle slip toward the upstream side of the dam. Conglomerates are cream to brown color and low to moderate strength, mainly composed of calcareous grains in a fine-grain

matrix with loose calcareous cement. Younger alluvial deposits of the river bed, with limited thickness, were removed during the construction phases and the dam foundation has been placed on the bedrock.

4.2. The Apparent Effects on Tange-Hamam Dam

Longitudinal cracks openings and relative settlement are the most important determinants of possible damages due to earthquake events [26-28]. After the earthquake, according to the low distance of the earthquake epicenter to the Tange-Hamam

Dam, visual inspections were carried out on the site. Observations revealed the occurrence of cracks with very small openings on the crest of the dam and also an upright crack in the concrete body of the spillway's left guide wall. Figure (4) shows the images of the mentioned cracks on the crest of the dam. Initial opening of the cracks in different locations of its length has been inspected and marked by nailing for post-earthquake monitoring. Further monitoring and inspection have been placed on the agenda that shows the stagnation and lack of growth in cracks.



Figure 4. Images of observed cracks in Tange-Hamam Dam, (a) General view of the dam after the earthquake, (b) very small tiny transversal crack on the crest, (c) Longitudinal Crack on the crest, and (d) Crack and separation on the concrete at a joint place of the left wall of the spillway.

4.3. Settlement of the Dam Body due to the Earthquake

In order to determine the amount of settlement in Tange-Hamam Dam, settlement measures of instrumentations in dam's body have been studied. Figure (5) shows the location and plan of instrumented sections of Tange-Hamam Dam. Settlement measure pipes of the dam body have been installed in sections 3, 5 and 7. At each section, there are two pipes, one at the core of the dam and one in the downstream shell. Figure (6) shows the position of settlement pipes of the core and the shell of the dam in different sections. Settlement measuring plates are from magnetic-type and the plates have been installed approximately at a 3 m distance. According to the embankment height, the numbers of the measuring plates are different in every station. The last plate of settlement measuring plates have been located in about 3 m distance of the surface and their settlement could be considered as the minimum settlement of the embankment surface. In every settlement pipe, the terminal measuring plate of the settlement, which located on the bed-rock, has been considered as the base point and the embankment settlement measured relative to this basis. Moreover, the position of settlement measuring plates at the end of the construction phase has been considered as the temporal basis to

measure the amounts of settlement during the time.

Figure (7) shows the amount of the settlement against time for every measuring plate of settlement. Plates numbering is from embankment depth to the ground surface. The graphs also show the date of the recent Sarpol-e Zahab earthquake event. As can be seen, the settlement rate in the initial period after the completion of the dam construction was significant, but gradually the settlement rate has been reduced. After about five years from the completion of the dam construction, the settlement rate was about zero and the amount of the calculated settlement in several readings before the earthquake event show approximately the same constant values. The largest amount of settlement occurred in the period between the completion of the dam and before the recent earthquake, was 58 centimeters in the middle section of the dam and in the plate located close to the crest.

After Sarpol-e Zahab earthquake occurrence, four settlement reading sessions have been performed in a week intervals. Although first reading after the earthquake is thoroughly different in comparison with earlier readings before the earthquake, the subsequent readings in the dam's body stayed relatively constant. The largest amount of settlement could be followed in the S-05-1 settlement measuring pipe, which is the only measurement that shows a small increasing trend in settlement readings and so needs to monitor its behavior in later sessions. Table (3) shows the relative settlement of the measuring plates close to the

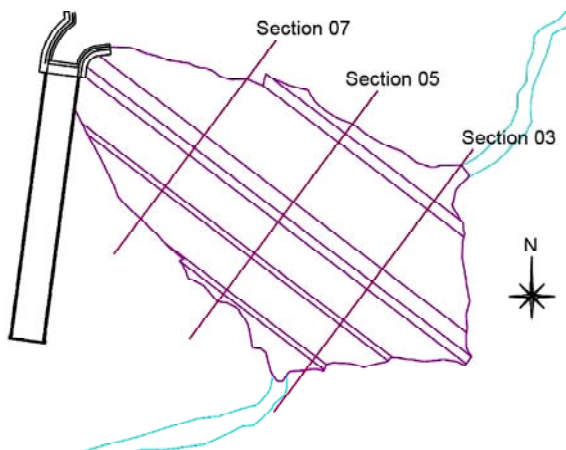


Figure 5. Plan of instrumented sections in Tange-Hamam Dam.

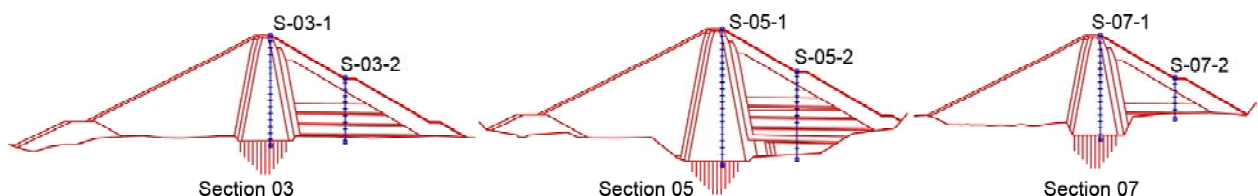


Figure 6. Location of the settlement pipes in the core and shell of the dam in different sections.

Table 3. Relative settlement near the embankment surface (in centimeters).

Settlement Pipe	Before EQ	After EQ	Due to EQ
S-03-1	51	58	6
S-03-2	24	25	1
S-05-1	58	71	13
S-05-2	24	28	4
S-07-1	51	58	7
S-07-2	11	11	0

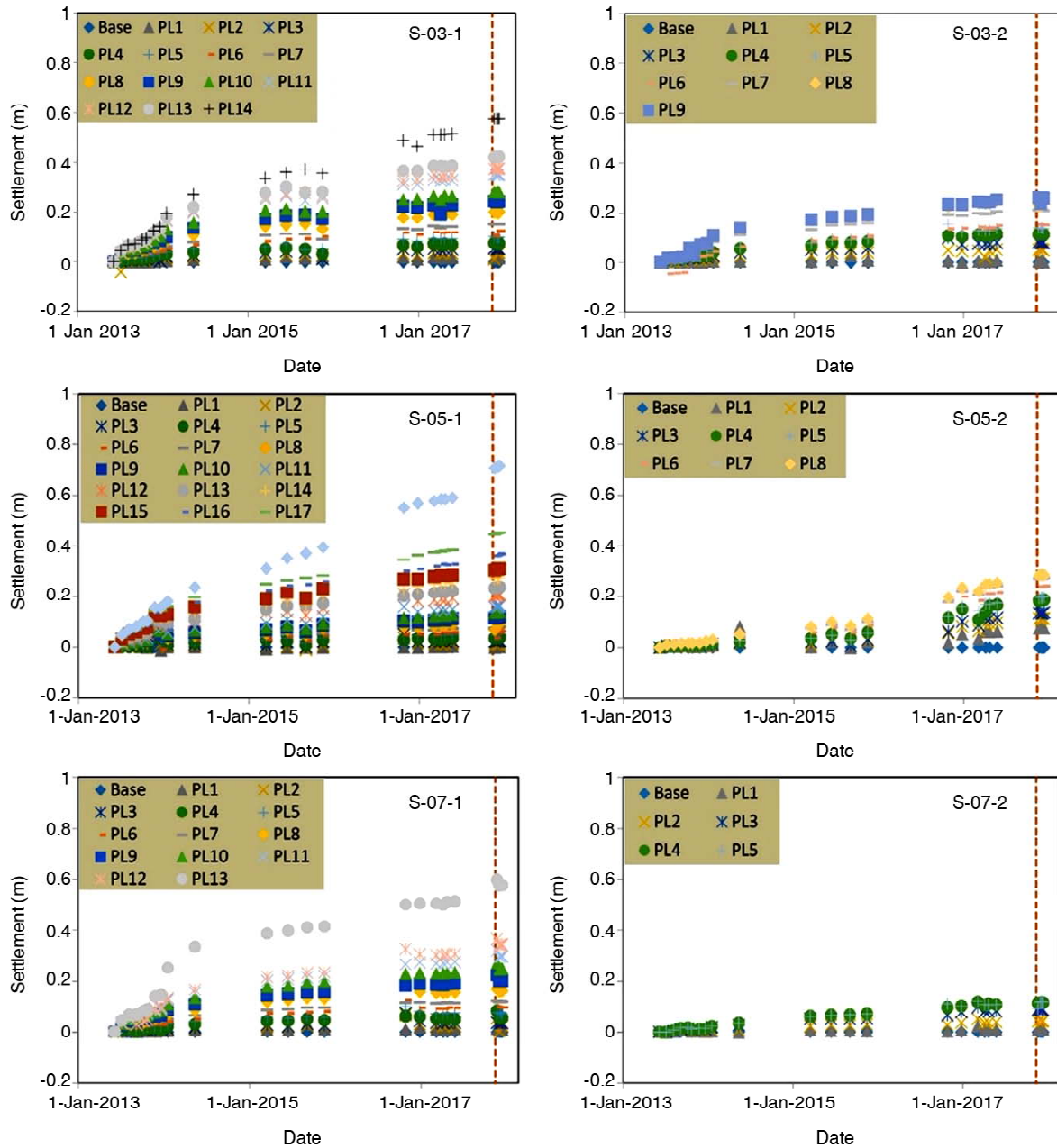


Figure 7. Settlement of the dam's body after the completion of the construction.

embankment surface, before and after the earthquake as well as their differences that means earthquake-related settlement. The relative settlement values were achieved by averaging from four readings of before and after the earthquake. The largest amount of settlement has been recorded in S-05-1 gauge as 13 cm. According to the 60 m height of the dam's body embankment, it would be equal to 0.22 percent of the total height of the dam.

Figure (8) contains the earthquake-related settlement values in terms of the level of the monitoring point. As it can be seen, the settlement in lower third of the dam, especially in the core

gauges is negligible and the highest amount of settlement occurs in upper third of the dam body in a way that at S-05-1, about 3 cm of total 13 cm occurred in the bottom two-thirds of the dam body and 10 cm occurred in upper third part. There is also a similar situation in S-03-1 and S-07-1 so that among the total settlement of 6 and 7 cm, respectively, less than 2 cm occurred in bottom two-thirds and the rest is related to the upper third part. The settlement gauges located on the sides of the shell, downstream of the dam, has negligible quantities and just the settlement gauge, which located in the middle section shows near 4 cm settlement close to the surface. At this point, unlike

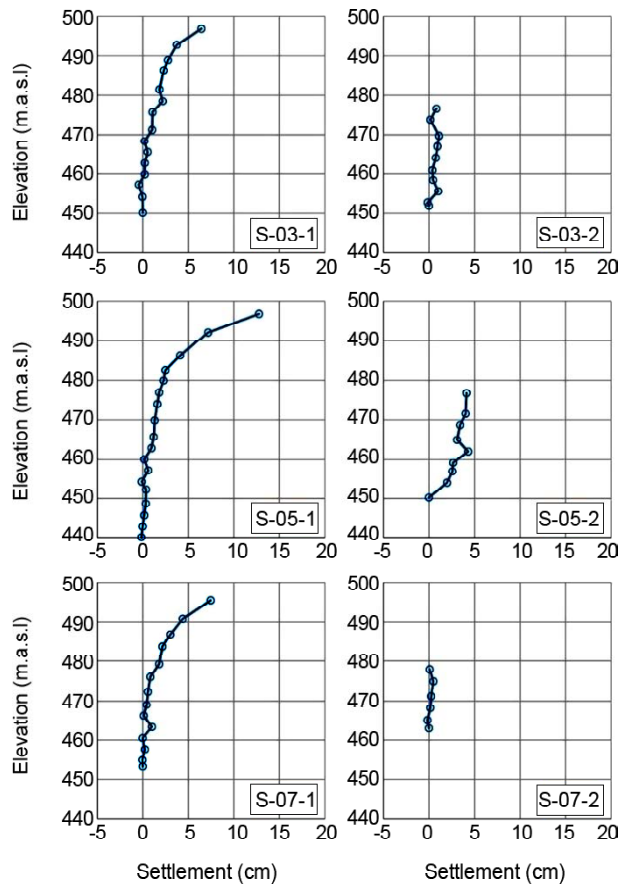


Figure 8. Earthquake-related settlement in different levels of the dam's body.

other gauges of the central core, settlement distribution in the body height is more uniform.

4.4. Evaluation of Settlement in Tange-Hamam Dam

Bureau et al. [29] introduced an earthquake intensity index chart to predict the earthquake-related settlement of rock-fill embankment dams. Earthquake Intensity index is introduced as follows:

$$ESI = PGA \cdot (M - 4.5)^3 \quad (1)$$

where *ESI* denotes earthquake intensity index, *PGA*, is peak ground acceleration in dam site (based on *g*), and *M* is the earthquake magnitude. Besides, Swaisgood [27-28] studied settlement in 54 earth-fill and rock-fill dams and proposed following relationship to predict earthquake-related settlement in dams:

$$NCS = EXP[5.70 PGA + 0.47 M - 7.22] \quad (2)$$

where *NCS* is a normalized settlement of the crown, *PGA* is peak ground acceleration in dam site, and *M* is the earthquake magnitude. For

assessment and prediction of the earthquake-related settlement in the body of the earth dams, the maximum ground acceleration is required at the site. Although the Tange-Hamam Dam has been equipped with accelerometers mounted on the dam and free field before the earthquake, the lack of proper operation has led to the lack of recording of acceleration during the earthquake. If the Mountain Front Fault considered as the earthquake-causative fault, due to the magnitude of the earthquake, this can be considered as the maximum credible earthquake of the site. The distance from this fault's outcrop to the site is less than 5 km, which was considered as the basis for maximum credible level (MCL) acceleration of the site in the dam studies. Table (4) shows the considered peak ground acceleration values for different hazard levels in Tange-Hamam Dam site during the design studies, where the peak ground acceleration for maximum credible level considered to be 0.6 *g*. Moreover, the estimation of peak ground acceleration in the dam site has been examined by use of the Next Generation Attenuation (NGA) relationships of Campbell and Bozorgnia [30], Abrahamson and Silva [31] and Chiou and Youngs [32]. Figure (9) shows the mentioned attenuation relationships for a

Table 4. Peak ground acceleration for Tange-Hamam Dam site (Abfan Consulting Engineer, 2012).

Seismic Level	Computation Method	Return Period	HPGA
DBL	Probabilistic	500	0.225
MDL	Probabilistic	2000	0.332
MCL	Deterministic	-	0.594

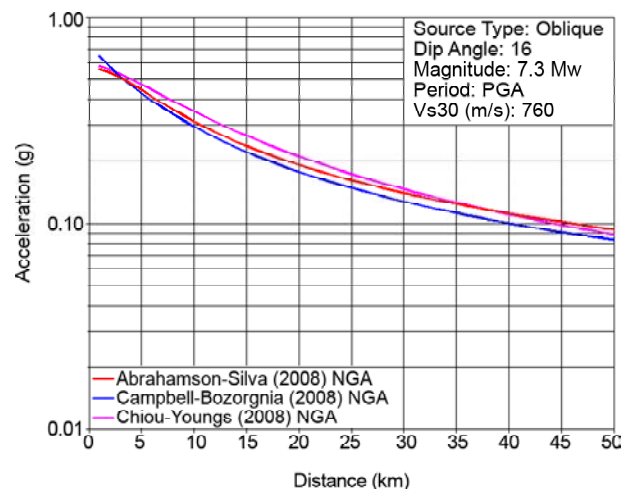


Figure 9. Attenuation of PGA based on NGA relationships for an earthquake with *M* = 7.3.

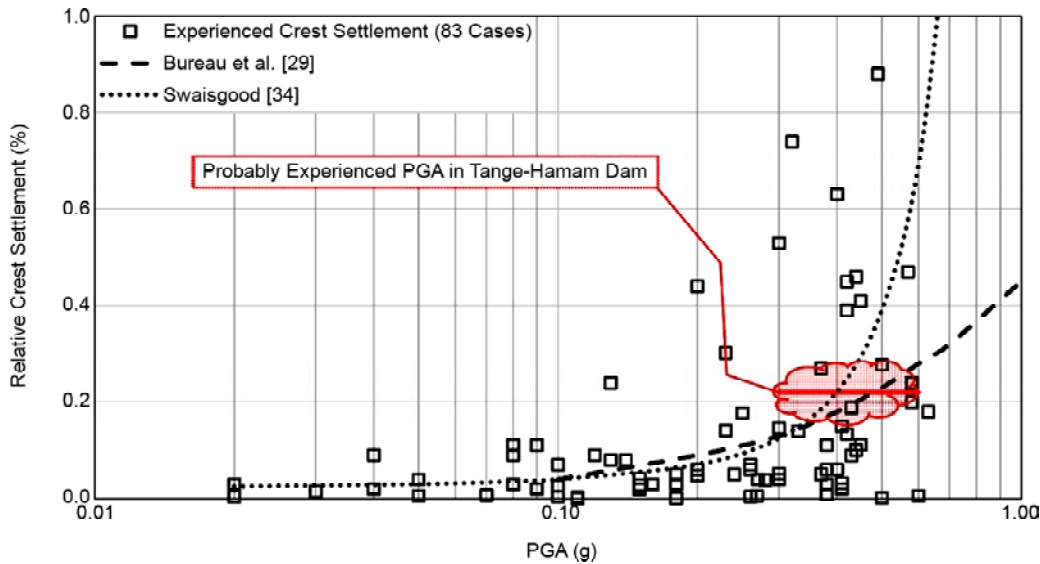


Figure 10. Comparison of settlement in Tange-Hamam Dam with world data and empirical relationships for an earthquake with $M=7.3$.

rock site in foot wall side of an oblique source with the dip angle of 16° and magnitude of 7.3 in terms of the rupture distance. As can be seen, all the presented relationships propose the PGA values of more than 0.3 g for distances less than 10 km to the site without considering the near-field effects. Accordingly, a PGA range between 0.3 g to 0.6 g can be considered for the dam site location.

Considering the peak ground acceleration of at least 0.3-0.6 g as the incident acceleration in the Tange-Hamam Dam site during the recent earthquake, the measured amount of earthquake-related settlement has been assessed and compared to the predicted values. The considered acceleration would not be unrealistic according to the acceleration of 0.68 g, which was recorded in Sarpol-e Zahab city [33] during the earthquake. Figure (10) shows the values of the earthquake-related settlement experienced in 83 embankment dams caused by 39 earthquakes since 1920 [34]. Besides, in the figure the earthquake-related settlement of Tange-Hamam Dam along with the predicted values of settlement, based on the empirical relationships of Bureau et al. [29], and Swaisgood [28] for an earthquake with the magnitude of 7.3, have been presented. As can be seen, if the peak ground acceleration in the Tange-Hamam Dam site considered as 0.3-0.6 g, the amounts of settlement occurred in the dam is in the range of the predicted values by experimental relationships, and it can be concluded that the Tange-Hamam Dam performance

was acceptable in total.

Particularly, the data which has been showed in Figure (10), contains 36 cases of dams which have experienced the PGA of 0.3 g to 0.6 g as it is expected for Tange-Hamam Dam that about half of them have been faced moderate to major damages during the earthquakes. Among them, The Upper San Fernando earth core rockfill dam, during February 9, 1971, ($M_w = 6.6$) earthquake, experienced the highest amount of settlement, which was 2.11 percent of the dam height due to a 0.55 g PGA. This dam showed a 1.02 percent settlement once more due to 0.42 g PGA of January 17, 1994 earthquake that was noticeable. Besides, Austrian Dam in California, which showed a 1.51 percent settlement due to a 0.57 g PGA during October 17, 1989 ($M_w = 7.1$) earthquake was another case that is worth to note. The Upper San-Fernando dam and Austrian dam constructions are finished in 1920 and 1950, respectively. When the modern construction rules were not still considered in the building of the dams. In conclusion, commitment to modern construction standards, resulted acceptable performance of Tange-Hamam dam during Sarpol-e Zahab ($M_w = 7.3$) earthquake.

5. Conclusion

After the Sarpol-e Zahab earthquake, an emergency inspection of operational dams at a radius of 125 km from the earthquake epicenter was carried out. Visually inspected dams have not

shown significant evidence of damages except for some small cracks. The Tange-Hamam Dam was the nearest dam to the earthquake epicenter by 25 km distance. Monitoring the situation of the cracks revealed that there are no significant changes to their extension after the earthquake. The earthquake-related settlement in Tange-Hamam Dam measured 13 cm in the middle section of the dam, which was equal to 0.22 percent of the height of the dam. A large part of this settlement occurred in the upper third of the dam and the settlement of the lower two-thirds was almost negligible. Comparison of the measured settlement with predicted values based on peak ground acceleration for the maximum credible level in Tange-Hamam Dam site, and also regarding historical experiences of settlements due to earthquake events, indicate the acceptable and suitable performance of the dam during and after the earthquake event. In general, all the dams affected by the Sarpol-e Zahab earthquake have had an acceptable and suitable performance.

References

1. Bollinger, G.A. (1977) 'Reinterpretation of the intensity data for the 1886 Charleston, South Carolina, earthquake'. In *Studies Related to the Charleston, South Carolina, Earthquake of 1886 - A Preliminary Report*. Rankin, D.W. (ed.), U.S. Geological Survey Professional Paper 1028, 17-32.
2. USCOLD (1992) *Observed Performance of Dams During Earthquakes, Volume I*. United States Society on Dams, 129p.
3. USCOLD (2000) *Observed Performance of Dams During Earthquakes, Volume II*. United States Society on Dams, 162p.
4. USCOLD (2014) *Observed Performance of Dams During Earthquakes, Volume III*. United States Society on Dams, 121p.
5. Tani, S. (2000) Behavior of large fill dams during earthquake and earthquake damage. *Soil Dynamics and Earthquake Engineering*, **20**, 223-229.
6. Seed, H.B., Lee, K.L., and Idriss, I.M. (1969) Analysis of Sheffield dam failure. *ASCE Journal of Soil Mechanics and Foundation Division*, **95**(SM6), 1453-1490.
7. Moriwaki, Y., Tan, P., and Ji, F. (1998) Seismic deformation analysis of the Upper San Fernando Dam under the 1971 San Fernando earthquake. *Proceeding of Geotechnical Earthquake Engineering and Soil Dynamics*, **III**, American Society of Civil Engineers, 854-865.
8. Seed, H.B., Lee, K.L., Idriss, I.M., and Makdisi, F.I. (1975) The slides in the San Fernando Dams during the earthquake of February 9, 1971. *Journal of the Geotechnical Engineering Division*, ASCE, **101**(GT7), 651-688.
9. Castro, G., Poulos, S.J., and Leathers, F.D. (1985) A re-examination of the slide of the lower San Fernando dam. *Journal of Geotechnical Engineering*, ASCE, **111**(GT9).
10. Krinitzky, E.L. and Hynes, M.E. (2002) The Bhuj, India, earthquake: lessons learned for earthquake safety of dams on alluvium. *Engineering Geology*, **66**, 163-196.
11. Singh, R., Roy, D., and Jain, S.K. (2005) Analysis of earth dams affected by the 2001 Bhuj Earthquake. *Engineering Geology*, **80**, 282-291.
12. Yamaguchi, Y., Kondo, M., and Kobori, T. (2012) Safety inspections and seismic behavior of embankment dams during the 2011 off the Pacific Coast of Tohoku earthquake. *Soils and Foundations*, **52**, 945-955.
13. Chen, G., Jin, D., Mao, J., Gao, H., Wang, Z., Jing, L., and Li, X. (2014) Seismic damage and behavior analysis of earth dams during the 2008 Wenchuan earthquake, China. *Engineering Geology*, **180**, 99-129.
14. Zhang, J.M., Yang, Z.Y., Gao, X.Z., and Zhang, J.H. (2015) Geotechnical aspects and seismic damage of the 156-m-high Zipingpu concrete-faced rockfill dam following the Ms 8.0 Wenchuan earthquake. *Soil Dynamics and Earthquake Engineering*, **76**, 145-156.
15. Biederman, R. (1985) *Dam safety in Switzerland, Swiss Dams - Monitoring and Maintenance*. Swiss National Committee on Large Dams, Switzerland.

16. Pougatsch, H., Müller, R.W., and Kobelt, A. (1998) Water alarm concept in Switzerland. *Proceedings of the International Symposium on new Trends and Guidelines on Dam Safety*, Barcelona, Spain, Berga ed. Balkema, Rotterdam, 235-242.
17. Emami, K. (2014) The historic kurit dam: An illustrative example of water wisdom. *Irrigation and Drainage*, **63**, 246-253.
18. ODSS (2013) *Guideline for Seismic Analysis and Design of Earth and Rockfill Dams*. Office of Deputy for Strategic Supervision, Dept. of Technical Affairs. Publication No. 624.
19. Hessami, K., Jamali, J., and Tabassi, H. (2003) *Major Active Faults of Iran*. Seismotectonic Department, Seismology Research Centre, International Institute of Earthquake Engineering and Seismology.
20. Hessami, K. and Jamali, J. (2006) Explanatory notes to the map of major active faults of Iran. *Journal of Seismology and Earthquake Engineering*, **8**(1), 1-11.
21. IBCS (2015) *Iranian Code of Practice for Seismic Resistant Design of Buildings, Standard No. 2800*. 4th Edition, Iranian Building Codes and Standards, Road, Housing and Urban Development Research Center.
22. ICOLD (1983) *Seismicity and Dam Design*. Bulletins No. 46, Committee on Seismic Aspects of Dam Design, International Commission on Large Dams, Paris.
23. ICOLD (1988) *Inspection of Dams Following Earthquakes - Guidelines*. Bulletins No. 62, Committee on Seismic Aspects of Dam Design, International Commission on Large Dams, Paris.
24. IRSC (2017) *Report on the November 12, 2017 M 7.3 Sarpol-e Zahab Kermanshah Earthquake*. Iranian Seismological Center, Institute of Geophysics, University of Tehran.
25. Abfan Consulting Engineer (2012) *Summary Report of Tange Hamam Storage Dam Project*. Report No: 86021-910601.
26. Pells, S. and Fell, R. (2003) Damage and cracking of embankment dams by earthquake and the implications for internal erosion and piping. *Proc. 21st Internal Congress on Large Dams*, Montreal, ICOLD, Paris Q83-R17, International Commission on Large Dams, Paris.
27. Swaisgood, J.R. (1998) Seismically-induced deformation of embankment dams. *Proc. U.S. National Conference on Earthquake Engineering*, Seattle, Washington.
28. Swaisgood, J.R. (2014) Behavior of embankment dams during earthquake. *Journal of Dam Safety, ASDSO*, **12**(2), 35-44.
29. Bureau, G., Volpe, R.L., Roth, W.R., and Udaka, T. (1985) Seismic Analysis of Concrete Face Rockfill Dams. *ASCE Int. Symp. on CFRD's, Detroit*, Oct. 21, in *Concrete Face Rockfill Dams - Design, Construction and Performance*, 479-508, and Closure (1987), *ASCE Journal of Geotechnical Eng. Div.*, **113**(10), 1255-1264.
30. Campbell, K.W. and Bozorgnia, Y. (2008) NGA ground motion model for the geometric mean horizontal component of PGA, PGV, PGD and 5% damped linear elastic response spectra for periods ranging from 0.01 to 10 s. *Earthquake Spectra*, **4**(1), 139-171
31. Abrahamson, N.A. and Silva W.J. (2008) Summary of the Abrahamson and Silva NGA ground-motion relations. *Earthquake Spectra*, **24**(1), 67-97.
32. Chiou, B.S.-J. and Youngs, R.R. (2008) An NGA model for the average horizontal component of peak ground motion and response spectra. *Earthquake Spectra*, **24**(1), 173-215.
33. Farzanegan, E., Pour Mohamad Shahvar, M., MirSanjari, M., Eshaghi, A., Abdollahi, H., and Mirzaei, H. (2017) *Preliminary Report of Accelerometer Network on the November 12, 2017 M 7.3 Sarpol-e Zahab Kermanshah Earthquake*. Iran Strong Motion Network, Road, Housing and Urban Development Research Center.
34. Swaisgood, J.R. (2003) Embankment dam deformations caused by earthquakes. *Proc. 2003 Pacific Conf. Earthq. Eng.*, **40**, 1-8.